09 Feb 2006

Wagging the Contact Line: Transverse and Longitudinal Waves

S. Saritha

Partho Neogi

Missouri University of Science and Technology, neogi@mst.edu

Wagging the contact line: Transverse and longitudinal waves

S. Saritha and P. Neogi[a)]
Chemical and Biological Engineering, University of Missouri-Rolla, Rolla, Missouri 65409-1230

(Received 10 November 2005; accepted 16 December 2005; published online 9 February 2006)

Kinetics of wetting has been explored where the contact line not only sees a steady spreading but also has longitudinal or transverse oscillations imposed on it. The latter case is realized when spreading takes place over a rough surface. The effects of the imposed motion are small, which seem to be due to low spreading rates and small dynamic contact angles used in this study. However, a singularity is seen in viscous dissipation during the movement on the model rough surface, which is interpreted here as an instability that is similar to Haines' jumps and stick-slip phenomena, with possible entrainment of the displaced fluid. This is the first time that all of these have been associated with each other. © *2006 American Institute of Physics*. [DOI: 10.1063/1.2166366]

INTRODUCTION

The study of equilibrium contact angles on a rough solid surface has a long history. Wenzel[1] and Cassie and Baxter[2] have analyzed the effect of increased interfacial area as well as the effect of air trapped in the surface roughness. Experiments support both changes in contact angles and air trapping at large roughness.[3] In recent years, there has been some interest in contact angles on patterned surfaces,[4] where the issue of air trapping remains important. Air trapping has an important role, as it reduces the viscous drag on the liquid as it moves on the solid.[5,6]

The interest here lies in understanding wetting kinetics on a rough surface. Bascom *et al.*[7] showed that on a scratched surface, liquid spread faster than on unscratched surface if the grooves ran in the direction of the flow, and slower when the grooves ran perpendicular to the flow. Neogi and Miller[8] assumed that a flow over a rough surface could be approximated as a flow over a porous medium, and for random roughness the variance of the surface profile could be related to the permeability of the porous medium. There are some works that look at the effects of grooves. The liquid flows through the grooves ahead of the bulk by capillary action, at a rate that depends on the radius of the groove.[9] In turn, it can be noted that the radius of the groove is proportional to the square root of the permeability. However, the model that uses only permeability loses the ability to distinguish types of grooves. In his study of flow over grooves, Hocking[10] obtained the same conditions of flow over porous media used by Neogi and Miller.[8] Hocking also considered the entrapment of a second fluid. Models differ by the manner in which the details of roughness affect the expression for the permeability. Most often the actual contact line is lost in the rough surface.

We consider a somewhat different case. If the roughness of the solid surface is low, the profile could be modeled as a sine wave. This is how Johnson and Dettre[11] have modeled the rough surface to explain contact angle hysteresis. It is important to note that the dynamic contact line on such a surface moves tangentially, but also shows an oscillatory motion in the perpendicular direction. It is precisely the effect of these fluctuations on the motion of the contact line that we are interested in.

Other than the transverse motion discussed above, the contact line can also be vibrated laterally. These longitudinal effects have been studied by Daniel *et al.*[12,13] In their case the perturbations are large and not only is the substrate vibrated, the drop sitting on the surface also receives significant body blows. The observed effects are sufficiently significant and we include in our analysis the case where the solid surface oscillates longitudinally.

These are difficult problems to solve, but de Gennes[14] has shown at least a class of problems that can be solved in a simple way. For a wedge advancing on a horizontal solid surface and kept in place by moving the substrate with a velocity U, the viscous dissipation is first calculated for the entire wedge to be

$$\Phi = \frac{3\mu U^2}{\alpha} \ln\left|\frac{1}{\varepsilon}\right|, \tag{1}$$

where $\varepsilon = \ell/L$, ℓ is the small cutoff length (in the x direction) and L is the macroscale of the problem, α is the apparent dynamic contact angle, and μ is the viscosity of the liquid. The cutoff is used to eliminate unbounded behavior in the fluid mechanical quantities at the contact line, and for a rough surface ε is proportional to the roughness.[8] The system is shown in Fig. 1. Lubrication theory approximation is used to obtain the details of the flow, which is applicable when the flow is slow and the liquid wedge is flat and thin. Under the lubrication theory, the film profile is flat and thin, such that only the tangential velocity can be considered and assumed to vary mainly in the direction normal to the film. In addition, the spreading velocities are assumed to be small. Now, the contact line region contains a thin precursor film which has the actual contact line. The film thickness is of "colloidal scale" of <100 nm, and not visible to microscopy (which has errors of ± 14 μm in linear measurements). According to de Gennes, the part of the surface work that is consumed by the viscous dissipation in the precursor film is that due to the

a)Electronic mail: neogi@umr.edu

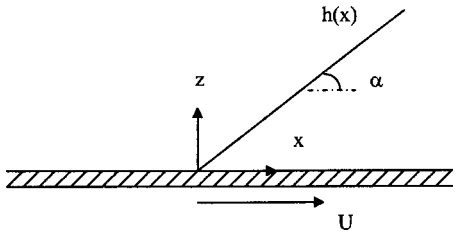

FIG. 1. Schematic view of a wedge on a horizontal solid substrate which moves with a velocity U. The coordinate system and the variables used have been shown as well as the contact angle α.

spreading coefficient S. The surface work that is consumed by viscous dissipation in the wedge is $U\gamma\alpha^2/2$, where γ is the surface tension and α is the angle of the wedge in Fig. 1 assumed to be small. The surface work is the scalar product between the velocity of the contact line and the effective force of surface tensions there. The angle of the wedge, α, is the angle measured using microscopy and is called the apparent dynamic contact angle since the term dynamic contact angle is reserved for the actual contact angle in absence of local equilibrium. However, we refer below to the apparent dynamic contact angle as the dynamic contact angle for convenience. For lubrication theory approximation to apply in the present case where the contact line (or the apparent contact line) experiences transverse or longitudinal vibrations, it is necessary to limit to low frequencies or low wave numbers.

We begin by noting that to measure reproducible contact angles, it is not very necessary to have specially smooth surfaces nor disturbance/vibration-free systems. (In contrast, the effect of contamination is critical.) That is, the effects studied below do not give rise to significant departures from ideal behavior. More features can be cited. Some experiments show that small and controlled vibrations actually improve reproducibility in contact angle measurements.[15,16] On rough surfaces, it appears that roughness changes contact angles only when the roughness is jagged, that is, the ratio between the amplitude and the wavelength is high.[17,18] Consequently, we expect that there is a feature which helps to dampen the effects of small roughness and vibrations, and it is important to identify why this happens. We are also interested in the analyses to find if exceptions happen. In fact, a striking exception, which provides a possible mechanism for air trapping, is obtained below.

LONGITUDINAL VIBRATIONS

de Gennes[14] equates the rate of viscous dissipation in Eq. (1) to the rate of surface work done $U\gamma\alpha^2/2$ to get

$$\alpha^3 = \frac{6\mu}{\gamma}\ln\left|\frac{1}{\varepsilon}\right| U. \tag{2}$$

For longitudinal vibrations of low frequency (ω), the inertial forces can be neglected. Thus, Eq. (2) remains unchanged,

$$U = U_0 + U_1 \sin \omega t. \tag{3}$$

Substituting Eq. (3) into Eq. (2) and rearranging,

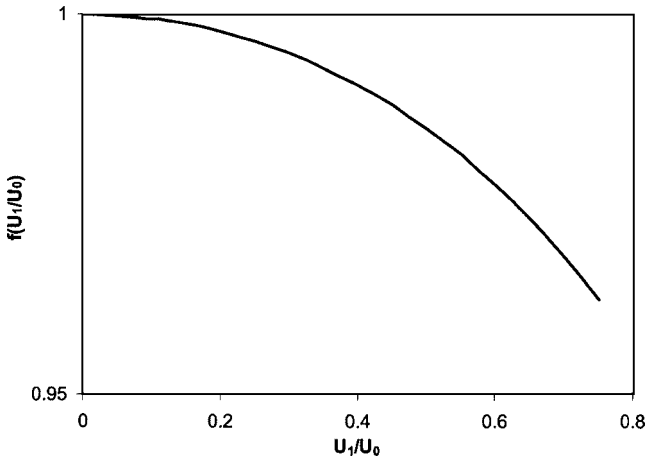

FIG. 2. The term in square brackets in Eq. (5), $f(U_1/U_0)$, has been shown as a function of U_1/U_0.

$$\alpha = \Lambda^{1/3}\left[1 + \frac{U_1}{U_0}\sin \omega t\right]^{1/3} \tag{4}$$

is obtained, where $\Lambda = (6\mu/\gamma)\ln|1/\varepsilon|U_0$. We average both sides of Eq. (4), where the average is $\langle\cdot\rangle = (\omega/2\pi)\int_0^{2\pi/\omega}\cdot\, dt$. It is difficult to carry out the integration analytically. For U_1/U_0 less than 1.0, a series expansion is performed, where the odd powers of the sine function become zero on averaging. We obtain

$$\langle\alpha\rangle = \Lambda^{1/3}\left[1 - \frac{1}{18}\left(\frac{U_1}{U_0}\right)^2 - \frac{5}{324}\left(\frac{U_1}{U_0}\right)^4 - \frac{385}{52488}\left(\frac{U_1}{U_0}\right)^6 \cdots\right], \tag{5}$$

with an error of the order of $(U_1/U_0)^8$. The result is independent of ω. For an error of order of ~ 0.1, the series is good to a large value of $U_1/U_0 \sim 0.75$. The term in square brackets has been plotted in Fig. 2 as a function $f(U_1/U_0)$. The effect is seen to be small. It is not necessary to assume that $U_1/U_0 < 1$ as long as ω is small. In the case where this ratio is 1 or more, the trend in Fig. 2 remains unchanged.

For nonwetting liquid, the surface work done has been shown to be[19] $U\gamma(\alpha^2 - \lambda^2)/2$ where λ is the equilibrium contact angle. Equating this to viscous dissipation, linearizing α about λ, we get

$$\lambda^2(\alpha - \lambda) = \frac{3\mu}{\gamma}\ln\left|\frac{1}{\varepsilon}\right|(U_0 + U_1 \sin \omega t). \tag{6}$$

We set U_0 to zero, that is, the substrate is vibrated about equilibrium. Thereafter, on averaging Eq. (6) the right-hand side is seen to be zero. That is, near equilibrium $\langle\alpha\rangle = \lambda$ in the presence of longitudinal vibrations.

TRANSVERSE OSCILLATIONS

The model for the flow over rough surfaces is shown in Fig. 3. Unlike Fig. 1, where the surface of the solid is at $z=0$, here the surface is at $z=s$, where $s = \alpha \sin(2\pi/\lambda)(x - Ut)$. Here, λ is the wavelength of the roughness and assumed to be large. Under lubrication theory approximation the flow is mainly in the tangential direction and varies

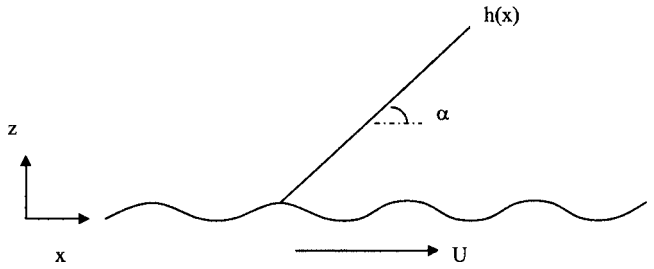

FIG. 3. A schematic view of a flow over a rough surface is shown with the coordinate system and key variables. The surface of the solid is at $z=s=a\sin(2\pi/\lambda)(x-Ut)$.

mainly in the perpendicular direction. For small velocities, quasistatic approximation can be used and the equation of motion becomes

$$0=\frac{\partial p}{\partial z}, \tag{7}$$

$$0=\mu\frac{\partial^2 v_x}{\partial z^2}-\frac{\partial p}{\partial x}, \tag{8}$$

where p is the pressure. This is solved subject to zero shear at $z=h$, the profile thickness, the no-slip boundary condition at $z=s$, and the zero flow rate, to obtain

$$v_x=U+\frac{3U}{(h-s)^2}\left(\frac{z^2}{2}-hz-\frac{s^2}{2}+hs\right). \tag{9}$$

The viscous dissipation becomes

$$\mu\left(\frac{\partial v_x}{\partial z}\right)^2=\frac{9U^2\mu}{(h-s)^4}(z-h)^2. \tag{10}$$

Integrating this from $z=s$ to $z=h$, we have

$$\phi=\int_s^h \mu\left(\frac{\partial v_x}{\partial z}\right)^2 dz=\frac{3\mu U^2}{(h-s)}. \tag{11}$$

Integrating ϕ from $x=\ell$ to $x=L$, we have

$$\Phi=\int_\ell^L \phi dx=3\mu U^2\int_\ell^L \frac{dx}{h-s}. \tag{12}$$

If in the integral, we set $s=0$ and $h=\alpha x$, Eq. (1) is obtained. On nondimensionalization we get

$$\Phi=3\mu U^2\int_{\ell/L}^1 \frac{d\xi}{\alpha\xi-\varepsilon\sin(2\pi/\Omega)(\xi-\tau)}, \tag{13}$$

where $\xi=x/L$, $\varepsilon=a/L$, $\tau=Ut/L$, and $\Omega=\lambda/L$. We also take ℓ, which is a dimension in the x direction, to be a/α since a is a dimension in the z direction. In using this cutoff, we take a view that the effective interface is along the tops of the roughness and the actual contact line is lost in the roughness, which is a view that is similar to those expressed in the initial discussion. At large times $\tau\gg\xi$ and on integrating by ignoring ξ in the presence of τ,

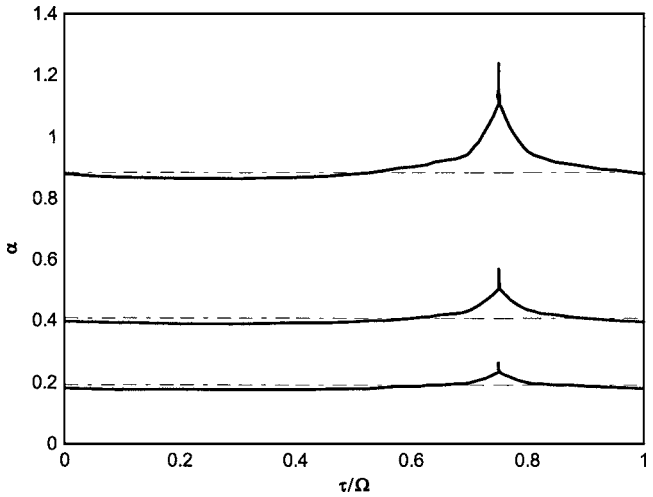

FIG. 4. A plot of α as it varies with τ/Ω for a single cycle has been shown for $\varepsilon=10^{-5}$, from Eq. (14). The values of capillary number Ca used are 0.01, 0.001, and 0.0001 from the top curve to the bottom curve as they appear on the graph. The dashed lines represent the results from Eq. (2).

$$\frac{\alpha^3}{6\mathrm{Ca}}=\ln\alpha+\ln\left|\frac{1}{\varepsilon}\right|-\ln\left[1+\sin\frac{2\pi\tau}{\Omega}\right] \tag{14}$$

is obtained where the capillary number $\mathrm{Ca}=\mu U/\gamma$. The term in logarithm of α is not very important. For $\varepsilon=10^{-5}$, we have calculated the values of α for one cycle, from τ/Ω of 0–1 for few values of Ca. The results are shown in Fig. 4. The variation in the values of α is not striking but there is a weak singularity at $\tau/\Omega=3/4$. For nonwetting liquids, α^3 is replaced with $\alpha(\alpha^2-\lambda^2)$. The results are shown in Fig. 5 in the form of α as a function of τ/Ω.

RESULTS AND DISCUSSION

The results for the longitudinal vibrations in Fig. 2 show that the effect of vibrations on the averaged value of the contact angles is low. This happens because the surface work

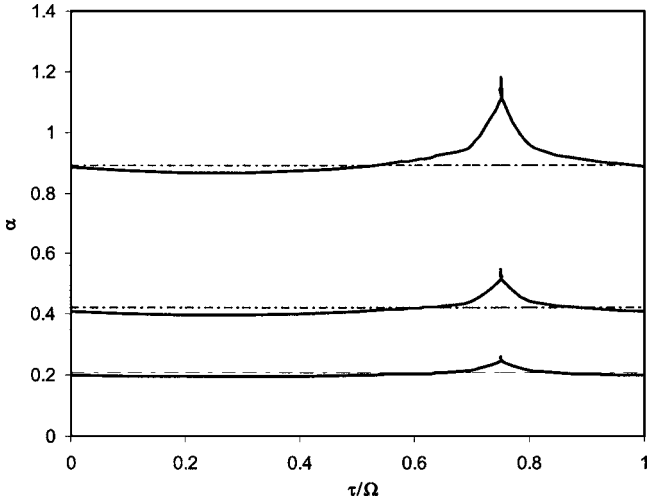

FIG. 5. A plot of α as it varies with τ/Ω for a single cycle has been shown for $\varepsilon=10^{-5}$ for the case of a nonwetting liquid, where α^3 in Eq. (14) is replaced with $\alpha(\alpha^2-\lambda^2)$. The values of capillary number Ca used are 0.01, 0.001, and 0.0001 from the top curve to the bottom curve as they appear on the graph. The dashed lines represent the results from Eq. (2).

is very strongly determined by the value of α (proportional to α^2). Smaller values of α indicate thinner films, and the films have been assumed to be thin throughout. As a result of this strong dependence a small change in α is equivalent to a large change in viscous dissipation. What we have done here is to change the rate of viscous dissipation, which as observed leads to only a small change in α. This is also the case in transverse vibrations as seen in Figs. 4 and 5. However, we note that this may not be the situation when α is large.

When longitudinal oscillations are given to the contact line of a nonwetting liquid originally at equilibrium, the result discussed after Eq. (6) shows that the average contact angle observed is the equilibrium value λ. This is in keeping with experimental observations[15,16] that controlled vibrations improve observations, although in those cases transverse oscillations are also included. No analogous results are available for rough surfaces.

The outstanding feature in the present results is the singularity in Figs. 4 and 5 at $\tau/\Omega=3/4$. Of course, the value of α cannot be unbounded. However, we note that in taking the profile to be $h=\alpha x$ we have made an approximation that under lubrication theory $\tan(\alpha)\approx\alpha$. If the tangent term is maintained, then the singularity only means that a value of $\alpha=\pi/2$ has been reached instead of a value of infinity, although it still lies well outside the range where the lubrication theory approximation is valid. Using the results from Figs. 4 and 5, it is possible to show that the viscous dissipation becomes singular at $\tau/\Omega=3/4$. The singularity is quite weak in Figs. 4 and 5. If the cutoff is increased, the singularity is replaced with a maximum, and the above interpretation appears to remain valid while showing that the effect of increased cutoff length decreases the role of the details of the surface roughness.

Johnson and Dettre[11] analyzed the case of a two-dimensional drop lying on a sinusoidal surface at equilibrium. Infinite configurations could be found subject to constant drop volume and a fixed microscale contact angle. The configurational energies were calculated and it was seen to have a maximum and a minimum for the foot of the drop lying inside a sinusoidal wave, and for every wave. Obviously, the maximum corresponds to an instability. Under dynamic situations, the foot of the drop will shoot forward until the unstable patch is skipped. These "violent" motions are called Haines' jump[20] and a less violent motion on a rough surface is called the stick-slip phenomenon.[21] The singularity in the viscous dissipation probably reflects the dynamic view of the equilibrium situation discussed earlier. These are the same as the contact line sigularity mentioned earlier, but it is localized; that is, on a rough surface some regions are negotiated differently than others. It can also be imagined that local equilibrium at the contact line does not hold during the jumps and can provide a mechanism where the displaced fluid/air gets trapped. Since the maximum energy is located near the bottom of the trough, the contact line would, in such a mechanism, hop over the trough. In the dynamic analog as well, the location of $\tau/\Omega=3/4$ implies $Ut=(3/4)\lambda$, that is, the effective contact line has moved to the bottom of a trough. We emphasize that in looking at the details of roughness, we get additional information of a very different kind as discussed in the Introduction. Compare this to the result that as the singularities in Figs. 4 and 5 are weak, α can be integrated to get an average value, which from the figures can be seen to be not very different from the results of Eq. (2) arrived at by assuming that the rough surface is the surface of a porous media.

If a randomly rough surface is characterized by peaks and troughs, then the present results will apply: the contact angles may not be affected by the details of the roughness; however, some roughness behind the contact line will not be irrigated just as some roughness ahead of the contact line are.[7]

ACKNOWLEDGMENT

This material is based on work supported by the National Science Foundation under Grant No. CTS-0228834.

[1] R. N. Wenzel, Ind. Eng. Chem. Res. **28**, 988 (1936).
[2] A. B. D. Cassie and S. Baxter, Trans. Faraday Soc. **3**, 16 (1944).
[3] R. E. Johnson, Jr. and R. E. Dettre, Adv. Chem. Ser. **43**, 136 (1964).
[4] N. A. Patankar, Langmuir **19**, 1249 (2003).
[5] M. Miwa, A. Nakajima, A. Fujishima, K. Hashimoto, and T. Watnabe, Langmuir **16**, 5754 (2000).
[6] J. Ou, B. Perot, and J. P. Rothstein, Phys. Fluids **16**, 4635 (2004).
[7] W. D. Bascom, S. L. Cottington, and C. R. Singleterry, Adv. Chem. Ser. **43**, 381 (1964).
[8] P. Neogi and C. A. Miller, J. Colloid Interface Sci. **92**, 338 (1983).
[9] R. R. Rye, J. A. Mann, Jr., and F. G. Yost, Langmuir **12**, 555 (1996).
[10] L. M. Hocking, J. Fluid Mech. **76**, 801 (1976).
[11] R. E. Johnson, Jr. and R. E. Dettre, Adv. Chem. Ser. **43**, 112 (1964).
[12] S. Daniel, M. K. Chaudhury, and P.-G. de Gennes, Langmuir **21**, 4240 (2005).
[13] S. Daniel, S. Sircar, J. Gliem, and M. K. Chaudhury, Langmuir **20**, 4085 (2004).
[14] P.-G. de Gennes, Acad. Sci., Paris., C. R. **298**, 111 (1984).
[15] W. Phillipoff, S. R. B. Cooke, and D. E. Caldwell, Min. Eng. **4**, 283 (1952).
[16] G. R. M. del Giudice, Eng. Mining J. **137**, 291 (1936).
[17] S. J. Hitchcock, N. T. Carroll, and M. G. Nicholas, J. Mater. Sci. **16**, 714 (1981).
[18] C.-M. Lin, R. M. Ybarra, and P. Neogi, Adv. Colloid Interface Sci. **67**, 185 (1996).
[19] F. Brochard-Wyart and P. G. de Gennes, Adv. Colloid Interface Sci. **39**, 1 (1992).
[20] G. L. Stegemeier, *Improved Oil Recovery by Surfactant and Polymer Flooding*, edited by D. O. Shah and R. S. Schechter (Academic, New York, 1977), p. 55.
[21] G. E. Elliott and A. C. Riddiford, J. Colloid Interface Sci. **23**, 389 (1967).